nature COMMUNICATIONS

ARTICLE

Received 4 Sep 2014 | Accepted 12 Feb 2015 | Published 24 Mar 2015

DOI: 10.1038/ncomms7629

Quantum dynamics of CO–H_2 in full dimensionality

Benhui Yang[1], P. Zhang[2], X. Wang[3], P.C. Stancil[1], J.M. Bowman[3], N. Balakrishnan[4] & R.C. Forrey[5]

Accurate rate coefficients for molecular vibrational transitions due to collisions with H_2, critical for interpreting infrared astronomical observations, are lacking for most molecules. Quantum calculations are the primary source of such data, but reliable values that consider all internal degrees of freedom of the collision complex have only been reported for H_2-H_2 due to the difficulty of the computations. Here we present essentially exact, full-dimensional dynamics computations for rovibrational quenching of CO due to H_2 impact. Using a high-level six-dimensional potential surface, time-independent scattering calculations, within a full angular momentum coupling formulation, were performed for the de-excitation of vibrationally excited CO. Agreement with experimentally determined results confirms the accuracy of the potential and scattering computations, representing the largest of such calculations performed to date. This investigation advances computational quantum dynamical studies representing initial steps towards obtaining CO–H_2 rovibrational quenching data needed for astrophysical modelling.

[1] Department of Physics and Astronomy and the Center for Simulational Physics, The University of Georgia, Athens, Georgia 30602, USA. [2] Department of Chemistry, Duke University, Durham, North Carolina 27708, USA. [3] Department of Chemistry, Emory University, Atlanta, Georgia 30322, USA. [4] Department of Chemistry, University of Nevada Las Vegas, Las Vegas, Nevada 89154, USA. [5] Department of Physics, Penn State University, Berks Campus, Reading, Pennsylvania 19610, USA. Correspondence and requests for materials should be addressed to P.C.S. (email: stancil@physast.uga.edu).

Quantum mechanical studies of inelastic processes in molecular collisions began with the development of the nearly exact, close-coupling (CC) method for rotational transitions in atom–diatom collisions by Arthurs and Dalgarno[1] and Takayanagi[2] in the 1960s. Over the past five decades tremendous advances in computational processing power and numerical algorithms have allowed high-level computations of inelastic processes[3,4], as well as reactive collisional dynamics of large molecular systems, the latter using primarily time-dependent approaches[5–7]. Until recently, however, the largest full-dimensional inelastic studies for a system of two colliding molecules have been limited to H_2-H_2 collisions in six-dimensions (6D), which were performed with both time-independent[8] and time-dependent[9,10] approaches for solving the Schrödinger equation. However, to make these computations possible, the authors resorted to various angular-momentum decoupling approximations with uncertain reliability. It was only recently[11–13] that these decoupling approximations were relaxed and essentially exact full-dimensional CC computations for the H_2-H_2 system became feasible. Despite the large internal energy spacing of H_2, which allows the basis sets to be relatively compact, these calculations are computationally demanding. Replacing one H_2 molecule with a molecule that has smaller internal energy spacing, such as carbon monoxide, would further increase the computational demands. Whether the CC method could in practice be used to describe such a diatom–diatom system in full dimensionality remains an open question.

First detected in the interstellar medium in 1970 (ref. 14), carbon monoxide is the second most abundant molecule, after H_2, in most astrophysical environments. CO has been the focus of countless theoretical astrophysical studies and observations, being detected in objects as distant as high redshift quasars[15] to cometary comae in our solar system[16] to the atmospheres of extrasolar giant planets[17]. Most studies have focused on pure rotational transitions observed in the far infrared to the radio or electronic absorption in the near ultraviolet. Over the past decade, however, near infrared emission of CO due to the fundamental vibrational band near 4.7 μm has been detected in a variety of sources including star-forming regions in Orion with the Infrared Space Observatory[18] and protoplanetary disks (PPDs) of young stellar objects[19–21] with the Gemini Observatory and the Very Large Telescope. In addition, pure rotational transitions, but in the first two vibrationally excited states ($v_1 = 1$ and 2), were detected by the Submillimeter Array in the circumstellar shell of the much-studied evolved star IRC + 10216 (ref. 22). In particular, high-resolution observations of the CO fundamental band probe the physical conditions in the inner disk region, ~10–20 astronomical units (AU), the site of planet formation. Detailed modelling of such environments requires state-to-state inelastic rovibrational excitation rate coefficients for CO due to H_2 collisions, but current simulations are limited to approximate scaling methods due to the dearth of explicit data[18,23].

In this Article, we address the two issues outlined above by advancing the state-of-the-art for inelastic quantum dynamics with a full-dimensional investigation using an accurate potential energy surface (PES) relevant to this scattering process, with a particular emphasis on the important region of the van der Waals complex. This was made possible through the accurate computation and precise fitting of a 6D CO–H_2 PES in the relevant region of the formaldehyde tetra-atomic system and the further development of the inelastic diatom–diatom time-independent scattering code, TwoBC[24], which performs full angular momentum coupling, the CC formalism[1], including vibrational degrees of freedom. We first briefly describe the new CO–H_2 PES and its testing through comparison of rotational excitation calculations using the 6D PES and 4D PESs (neglecting vibrational motion) and available experimental results. The full-dimensional (6D), essentially exact, computations for rovibrational quenching of CO($v_1 = 1$) due to H_2 collisions are presented resolving a two-orders-magnitude discrepancy between earlier 4D calculations, which adopted various approximations[25–28]. Finally, the current results are shown to be consistent with the rovibrational quenching measurements for the CO–H_2 system, performed at the Oxford Physical Chemistry Laboratory from 1976–1993, which no prior calculation has yet been able to adequately explain[29–31].

Results

The CO–H_2 PES. The CO–H_2 interaction has been of considerable interest to the chemical physics community for many decades with one of the first 4D surfaces for the electronic ground state constructed by Schinke *et al.*[32], which was later extended by Bačić *et al.*[25] The group of Jankowski and Szalewicz[33] performed accurate 5D and 6D electronic energy calculations, but averaged over monomer vibrational modes, and performed several fits to obtain a series of 4D rigid-rotor surfaces, referred to as the V98 (ref. 33), V04 (ref. 34) and V12 (ref. 35) PESs. A 6D PES for formaldehyde was constructed earlier by Zhang *et al.*[36], but it was developed for reactive scattering applications and, consequently, limited attention was given to the long-range CO–H_2 van der Waals configuration. Therefore, as a prerequisite to 6D inelastic dynamics studies, we carried out an unprecedented potential energy calculation including over 459 756 energy points (see Methods for details). The potential energy data were then fit using the invariant polynomial method with Morse-type variables in terms of bond-distances[37,38]. The resulting 6D PES, referred to as V6D, is shown in Fig. 1 for one sample configuration. Some features of V6D are also illustrated in Supplementary Figs 2–4.

Cross-sections and rate coefficients. Time-independent quantum scattering calculations were performed using the CC formulation of Arthurs and Dalgarno[1] as implemented for diatom–diatom collisions in the 4D rigid-rotor approximation in MOLSCAT[39] and extended to full-dimensional dynamics as described by Quéméner, Balakrishnan, and coworkers[12,13] in TwoBC. In the first set of scattering calculations, the new 6D PES was tested for pure rotational excitation from CO($v_1 = 0, j_1 = 0,1$), where v_1 and j_1 are the vibrational and rotational quantum numbers, respectively. The crossed molecular beam experiment of Antonova *et al.*[40], who obtained relative state-to-state rotational inelastic cross-sections, is used as a benchmark. The experimental cross-sections were determined at three centre of mass kinetic energies (795, 860 and 991 cm^{-1}), but with an initial state distribution of CO estimated to be 75 ± 5% for $j_1 = 0$ and 25 ± 5% for $j_1 = 1$. Antonova *et al.*[40] normalized the relative cross-sections to rigid-rotor calculations done with MOLSCAT using the V04 PES of Jankowski and Szalewicz[33]. Comparison of the experiment with new 4D rigid-rotor calculations on V12 and full-dimensional calculations on V6D are shown in Fig. 2. We find no difference in the excitation cross-sections when using V04 or V12, while the root mean square (RMS) cross-section errors between the normalized experiment and the V12 and V6D calculations range from $0.56–0.89 \times 10^{-16}$ cm^2 to $0.55–0.95 \times 10^{-16}$ cm^2, respectively (See Supplementary Table 1 and Supplementary Note 1). Clearly, a 4D rigid-rotor treatment of the dynamics is sufficient for describing rotational excitation at these relatively high energies.

The importance of full dimensionality for rotational excitation becomes more evident as the collision energy is reduced (see

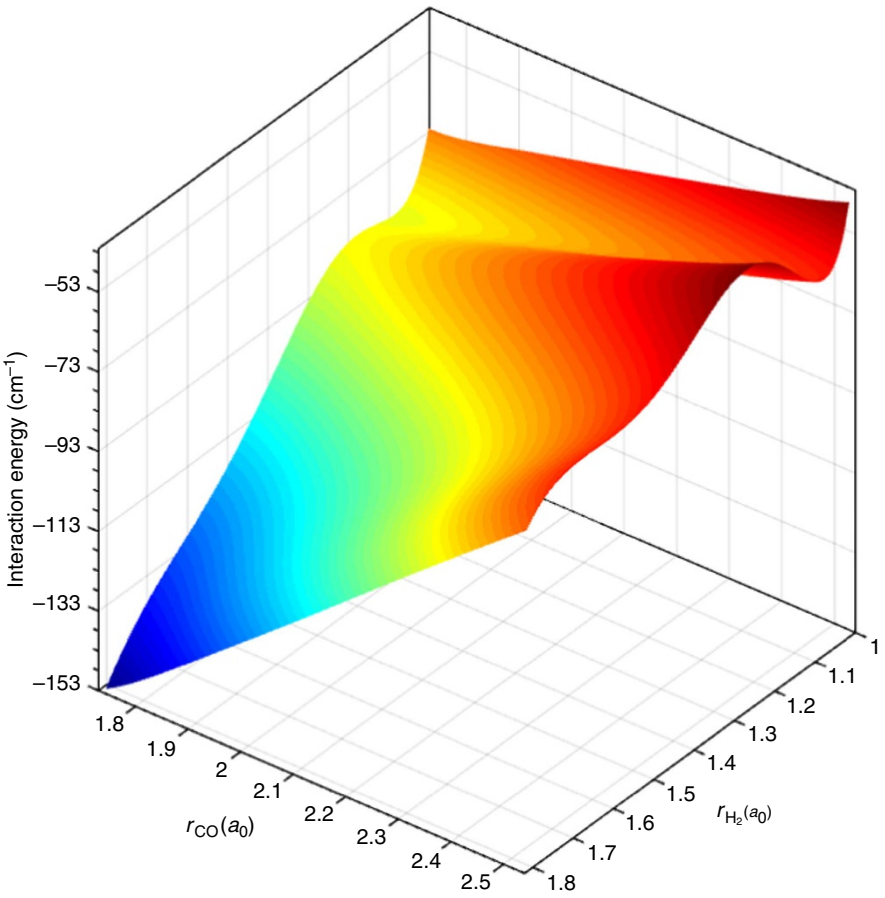

Figure 1 | The CO-H_2 interaction potential energy surface V6D. The potential surface is constructed in the 6D diatom–diatom Jacobi coordinates $(R,r_1,r_2,\theta_1,\theta_2,\phi)$, r_1 and r_2 are bond lengths, R the internuclear distance between CO and H_2 centre of masses, θ_1 and θ_2 the angles between **R** and $\mathbf{r}_1$ and $\mathbf{r}_2$, and ϕ the dihedral or twist angle. See Supplementary Figure 1. Here the dependence of the potential surface on bond lengths $r_{CO}=r_1$ and $r_{H2}=r_2$ is shown with $R=8$ a_0, $\theta_1=180°$, $\theta_2=0$ and $\phi=0$. Note that the CO(r_1) and H_2(r_2) diatom potentials have been subtracted.

also Supplementary Figs 5 and 6). Low-energy excitation cross-sections for the process

$$\mathrm{CO}(v_1=0,j_1=0)+\mathrm{H_2}(v_2=0,j_2=0) \rightarrow \mathrm{CO}(v_1'=0,j_1'=1)+\mathrm{H_2}(v_2'=0,j_2'=0), \quad (1)$$

or (0000)→(0100), using the notation defined in Methods, were measured by Chefdeville *et al.*[41] in a crossed-beam experiment. They obtained the excitation cross-section for centre of mass kinetic energies from 3.3 to 22.5 cm^{-1}. Although their energy resolution was limited, three broad features were detected near 6, 13 and 16 cm^{-1} attributed to orbiting resonances. Computed cross-sections for process (1) using the 4D V12 PES and the full-dimensional V6D PES are presented in Fig. 3a. While both computations reveal numerous resonances, the resonances are generally shifted by 2-3 cm^{-1} between calculations. The energy and magnitude of the resonances are very sensitive to the details of the PESs, but differences may also be due to the relaxation of the rigid-rotor approximation with the use of V6D in TwoBC. In Fig. 3b, the two calculations are convolved over the experimental energy resolution and compared with the measured relative cross-sections. Except for the peak near 8 cm^{-1}, the current 6D calculation appears to reproduce the main features of the experiment. RMS errors are found to be 0.355 and 0.228×10^{-16} cm^2 for the V12 and V6D PESs, respectively. Further details on the rotational excitation calculations can be found in Supplementary Note 1.

Now that the improved performance of the V6D potential for pure rotational excitation is apparent, we turn to rovibrational transitions. As far as we are aware, previous experimental[29–31,42,43] and theoretical[25–28] studies are limited to the total quenching of CO($v_1=1$). In the scattering calculations of both Bačić *et al.*[25,26] and Reid *et al.*[27], the 4D potential of Bačić *et al.*[25] was adopted, in which two coordinates were fixed ($r_2=1.4$ a_0, $\phi=0$), and various combinations of angular-momentum decoupling approximations for the dynamics were utilized (for example, the infinite order sudden, IOS, and coupled-states, CS, approximations; see Supplementary Note 2). More recently, Flower[28] performed CC calculations on a parameterization of the 4D PES of Kobaysashi *et al.*[44] These four sets of 4D calculations for quenching due to para-H_2 ($j_2=0$) are compared in Fig. 4 with the current 6D/CC calculations on the V6D surface for the case of $j_2=j_2'=0$. Corresponding state-to-state and total cross-sections for collisions with ortho-H_2 are given in Supplementary Figs 7–9 with further details in Supplementary Note 2.

A cursory glance at Fig. 4 reveals a more than two-orders-of-magnitude discrepancy among the various calculations. The large dispersion for the previous calculations is due to a combination of reduced dimensionality and decoupled angular momentum, which makes it difficult to assess the reliability of each approximation. The current results, however, remove these uncertainties by utilizing (i) a full-dimensional (6D) PES, (ii) full-dimensional (6D) dynamics and (iii) full angular momentum coupling. The sharp peaks in the cross-sections over the 1–10 cm^{-1} range in the 6D/CC results are due to resonances[45,46] supported by the CO–H_2 van der Waals potential well. These resonances, in the rovibrational quenching

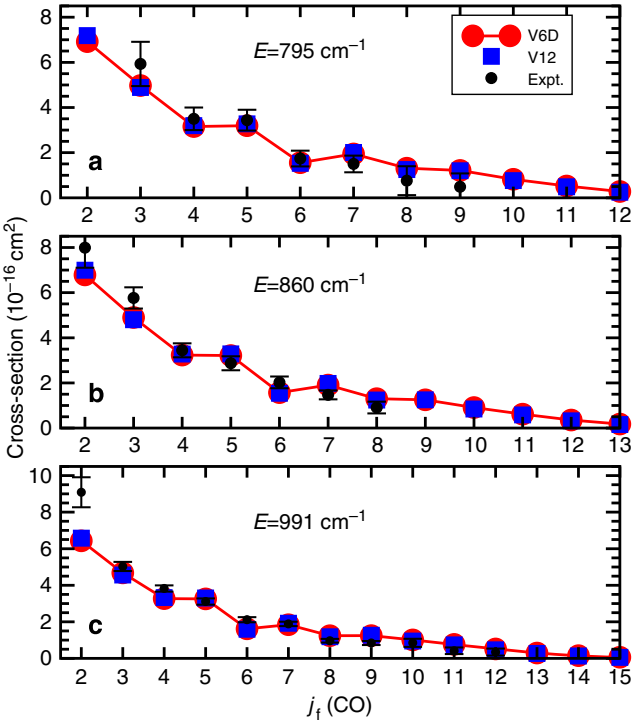

Figure 2 | State-to-state cross-sections for rotational excitation of CO($v_1=0,j_1=0,1$) by collisions with H_2. Theoretical results of full-dimensional calculations on V6D and 4D rigid-rotor calculations on V12 are compared with normalized experimental results[40] for collision energies of (**a**) 795 cm^{-1}, (**b**) 860 cm^{-1} and (**c**) 991 cm^{-1}. The calculations were performed for $H_2(v_2=0,j_2=0)$, but the experimental H_2 rotational distribution was undetermined. The error bars correspond to twice the estimated s.d. in the weighted means of the measurements[40].

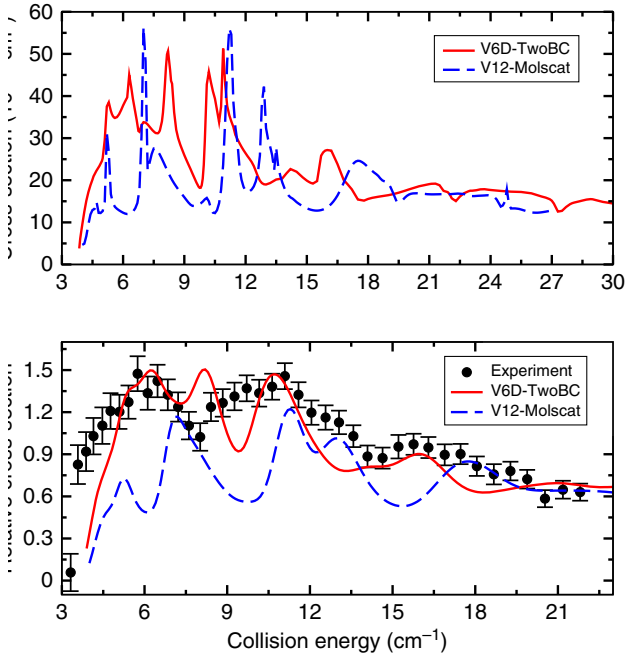

Figure 3 | Low-energy excitation cross-sections. $j_1=0 \rightarrow 1$ cross-sections for CO($v_1=0$) due to collisions with $H_2(v_2=0,j_2=0)$ are shown as a function of collision energy. (**a**) Computed cross-sections using the 4D V12 and 6D V6D PESs. (**b**) Computed cross-sections convolved over the experimental beam energy spread (lines) compared with the relative experiment of Chefdeville *et al.*[41] (circles with error bars). The error bars on the experimental cross-sections of Chefdeville *et al.* represent the statistical uncertainty at a 95% confidence interval.

of CO by H_2, are reported here for the first time and their prediction is made possible through our high-level treatment of the dynamics. Computations for transitions involving other initially excited j_2 states and inelastic H_2 ($j_2 \neq j_2'$) transitions are presented and compared in Supplementary Figs 10 and 11 and Supplementary Note 2.

Using the current 6D/CC cross-sections and the 4D/IOS-CS results of Reid *et al.*, rate coefficients for a Maxwellian velocity distribution are computed and compared in Fig. 5 with total de-excitation measurements[29–31] reported by Reid *et al.*[27] The comparison is not straight forward because (i) the measurements correspond to an initial thermal population of H_2 rotational states, (ii) the initial rotational population of CO($v_1=1,j_1$) was unknown, (iii) the experimental rate coefficients for ortho-H_2 are estimated from para- and normal-H_2 measurements and (iv) the contribution from a quasi-resonant channel,

$$\mathrm{CO}(v_1=1)+\mathrm{H_2}(v_2=0,j_2=2) \rightarrow \mathrm{CO}(v_1'=0)+\mathrm{H_2}(v_2'=0,j_2'=6)+\Delta E, \qquad (2)$$

dominates the para-H_2 case for $T \gtrsim 50$ K. Figure 5a displays the CO($v_1=1$) rovibrational de-excitation rate coefficients from the current 6D/CC calculations for collisions of ortho-H_2 for $j_2=1$ and 3, separately. These rate coefficients are summed over all j_1' and $j_2'=1$, 3 and 5. Assuming a Boltzmann average at the kinetic temperature T of the H_2 rotational levels $j_2=1$ and 3, presumed to be representative of the experimental conditions, rate coefficients are computed and found to be in good agreement with the measurements above 200 K. From Fig. 5a, the contribution from $j_2=3$ is seen to be only important above 150 K. The remaining difference with experiment at low temperatures may be due to the fact mentioned above that the ortho-H_2 rate coefficients are not directly measured, but deduced from normal-H_2 and para-H_2 experiments. In particular, Reid *et al.*[27] assume that the ortho/para ratio in the normal-H_2 measurements is 3:1, that is, statistical, and independent of temperature. Further, as stated above, the experimental CO rotational population distribution in $v_1=1$ is unknown. Nevertheless, the current 6D/CC computations are a significant advance over the 4D results of Reid *et al.*[27], which also correspond to a Boltzmann average of rate coefficients for $j_2=1$ and 3.

As indicated above, the situation for para-H_2 collisions is more complicated due to the quasi-resonant contribution (2), a mechanism not important for ortho-H_2. Boltzmann-averaged rate coefficients are presented in Fig. 5b including $j_2=0$ and 2 summed over $j_2'=0$, 2 and 4, with and without the quasi-resonant contribution, $j_2=2 \rightarrow j_2'=6$. While the current 6D/CC results and the 4D calculations of Reid *et al.*[27] are in agreement that the quasi-resonant contribution becomes important for $T \gtrsim 50$ K, the relative magnitude compared with the non-resonant transitions from the 6D/CC calculation is somewhat less than obtained previously with the 4D potential. This is partly related to the fact that the 6D/CC rate coefficients for $j_2=0$ are significantly larger than those of Reid *et al.*[27] (see also the corresponding cross-sections in Fig. 4 and in the Supplementary Fig. 9). Compared with the experiment, we obtain excellent agreement for $T \lesssim 150$ K, but are somewhat smaller at higher temperatures. This small discrepancy may be related to the unknown CO($v_1=1,j_1$) rotational population in the measurement. Nevertheless, it is only the 6D/CC computations, that is, dynamics in full dimensionality with full angular

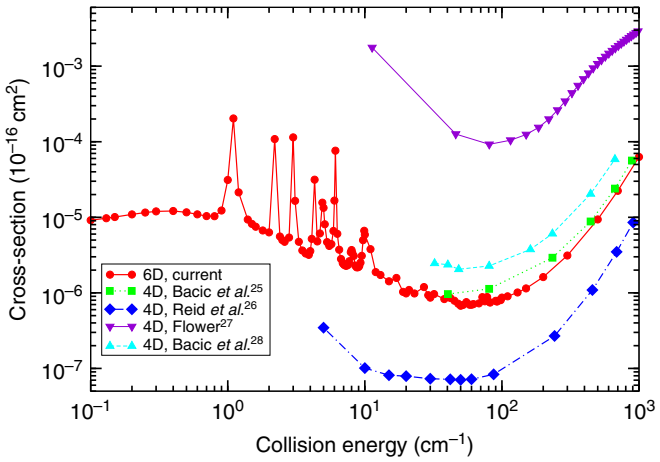

Figure 4 | Total theoretical cross-sections for the vibrational de-excitation of CO($v_1=1$) by para-H_2. Current 6D/CC results are compared with previous 4D calculations. The 4D results of Bačić *et al.*[26] and Reid *et al.*[27] do not distinguish CO rotational states, while the 4D results of Bačić *et al.*[25], 4D results of Flower[28], and the current 6D/CC results are for initial $j_1=0$ summed over all final CO($v_1'=0, j_1'$). In every case, the H_2 rovibrational state remains unchanged, $v_2, j_2 = v_2', j_2' = 0, 0$.

momentum coupling, that can reproduce the measurements for both ortho- and para-H_2. Further, the computations for the quasi-resonant process (2) were the most challenging reported here due to the requirement of a very large basis set (see Supplementary Table 2), which resulted in long computation times, a large number of channels and usage of significant disk space ($\sim$0.5 TB per partial wave). In total, the cross-sections given here consumed $>$40,000 CPU hours.

Discussion

The current investigation of the CO–H_2 inelastic collision system has been performed with the intent of minimal approximation through the computation of a high-level PES, robust surface fitting and full-dimensional inelastic dynamics with full angular momentum coupling. That is, within this paradigm for studying inelastic dynamics, we have advanced the state-of-the-art for diatom–diatom collisions through this unprecedented series of computations. The approach has been benchmarked against experiment for pure rotational and rovibrational transitions giving the most accurate results to date within the experimental uncertainties and unknowns. The accuracy and long-range behaviour of the 6D PES is found to be comparable to previous, lower-dimensional surfaces. The agreement of the current computation for the CO($v_1=1$) rovibrational quenching with

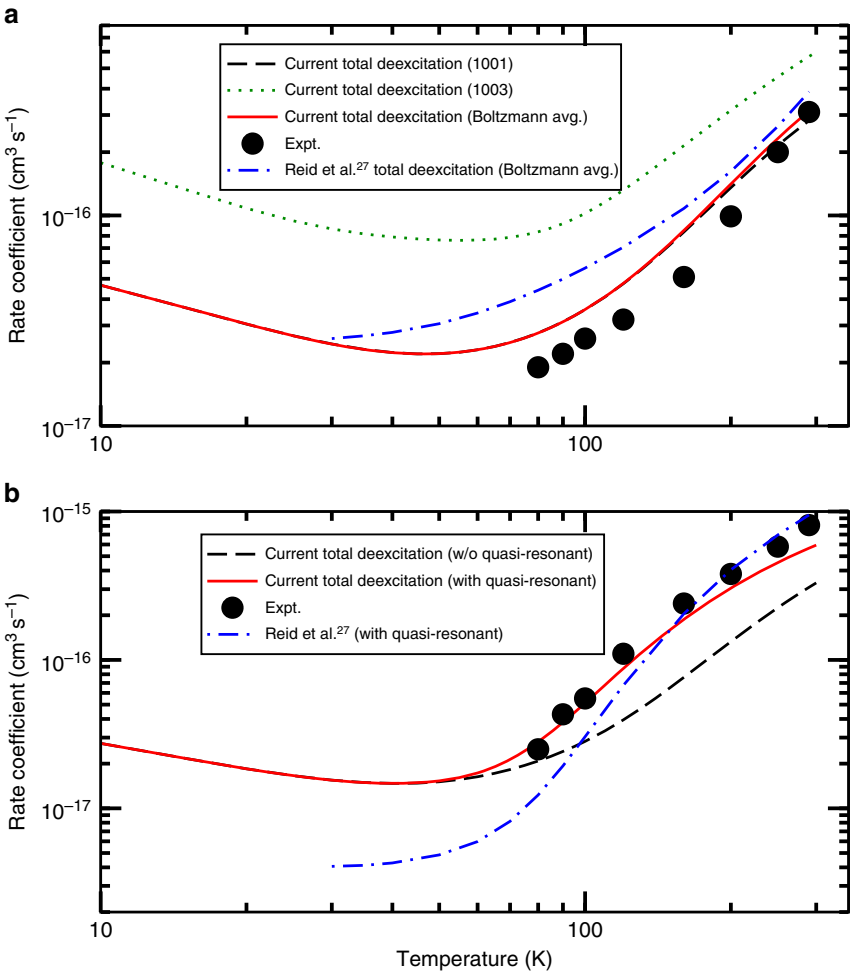

Figure 5 | Rate coefficients for the vibrational de-excitation of CO($v_1=1$) due to H_2. Current 6D/CC (solid, dashed and dotted lines) and Reid *et al.*[27] 4D (dot-dashed line) calculations are compared with the total CO($v_1=1$) rovibrational quenching experiment (symbols)[29–31]. (**a**) Ortho-H_2 rate coefficients for initial state-resolved, $(100\,j_2) \rightarrow (0j_1'0j_2')$, summed over j_1' and j_2' (dashed and dotted lines) and for a Boltzmann average of initial $H_2(j_2=1,3)$ (solid and dot-dashed lines). (**b**) Para-H_2 rate coefficients for a Boltzmann average of initial $H_2(j_2=0,2)$ with and without the quasi-resonant process (2). Note that the experimental uncertainties are smaller than the symbol sizes.

measurement resolves a long-standing (more than two-decades) discrepancy and justifies the requirement of a full-dimensional approach. This methodology can now, though with significant computational cost, be applied to a large range of initial rotational levels for $v_1 = 1$ and for higher vibrational excitation to compute detailed state-to-state cross-sections unobtainable via experiment.

This advance in computational inelastic scattering is particularly timely as ground-based (for example, the Very Large Telescope (VLT)) observations have focused on CO rovibrational emission/absorption in a variety of astrophysical objects, while related observations are in the planning stages for future space-based telescopes (for example, NASA's James Webb Space Telescope). In particular, we are in an exciting era of investigation into the properties of PPDs around young stellar objects[47]. PPDs provide the material for newly forming stars and fledgling planets. The CO fundamental band ($|\Delta v_1| = 1$) is a tracer of warm gas in the inner regions of PPDs and, with appropriate modelling, gives insight into disk-gas kinematics and disk evolution in that zone where planets are expected to be forming. A recent survey of 69 PPDs with the VLT[19] detected CO vibrational bands in 77% of the sources including $v_1 = 1 \rightarrow 0$, $v_1 = 2 \rightarrow 1$, $v_1 = 3 \rightarrow 2$, and even $v_1 = 4 \rightarrow 3$ in a few cases. Remarkably, rotational excitation as high as $j_1 = 32$ was observed. However, the modelling of PPDs, and other astrophysical sources with CO vibrational excitation, is hindered by the lack of rate coefficients due to H_2 collisions. We are now in an excellent position to provide full-dimensional, state-to-state CO–H_2 collisional data, which will not only have a profound impact on models characterizing these intriguing environments that give birth to planets, but also aid in critiquing current theories used to describe their evolution.

Methods

Potential energy computations. The potential energy computations were performed using the explicitly correlated coupled cluster (CCSD(T)-F12b) method[48,49], as implemented in MOLPRO2010.1 (ref. 50). The cc-pcvqz-f12 orbital basis sets[51] that have been specifically optimized for use with explicitly correlated F12 methods and for core-valence correlation effects have been adopted. Density fitting approximations[49] were used in all explicitly correlated calculations with the AUG-CC-PVQZ/JKFIT and AUG-CC-PWCVQZ-MP auxiliary basis sets[52,53]. The diagonal, fixed amplitude 3C(FIX) ansatz was used, which is orbital invariant, size consistent, and free of geminal basis set superposition error (BSSE)[54,55]. The default CCSD-F12 correlation factor was employed in all calculations, and all coupled cluster calculations assume a frozen core (C:1 s and O:1 s). The counter-poise (CP) correction[56] was employed to reduce BSSE. Although the explicitly correlated calculations recover a large fraction of the correlation energy, the CP correction is still necessary, mainly to reduce the BSSE of the Hartree–Fock contribution. Benchmark calculations at the CCSD(T)-F12b/cc-pcvqz-f12 level were carried out on selected molecular configurations and results were compared with those from the conventional CCSD(T) method using aug-cc-pV5Z and aug-cc-pV6Z basis sets. Results showed that the CP-corrected interaction energy agrees closely with those derived from CCSD(T)/aug-cc-pV6Z.

To construct the PES, the computations were performed on a six-dimensional (6D) grid using Jacobi coordinates as shown in Supplementary Fig. 1. R is the distance between the centre of mass of CO and H_2. r_1 and r_2 are the bond lengths of CO and H_2, respectively. θ_1 is the angle between $\mathbf{r}_1$ and $\mathbf{R}$, θ_2 the angle between $\mathbf{r}_2$ and $\mathbf{R}$, and ϕ the out-of-plane dihedral or twist angle. In the potential energy computations, the bond lengths are taken over the ranges $1.7359 \leq r_1 \leq 2.5359$ a_0 and $1.01 \leq r_2 \leq 1.81$ a_0, both with a step-size of 0.1 a_0. For R, the grid extends from 4.0 to 18.0 a_0 with step-size of 0.5 a_0 for $R < 11.0$ a_0 and 1.0 a_0 for $R > 11.0$ a_0. All angular coordinates were computed with a step-size of 15° with $0 \leq \theta_1 \leq 360°$ and $0 \leq \theta_2, \phi \leq 180°$. Additional points were added in the region of the van der Waals minimum.

The PES fit. The CO–H_2 interaction PES has been fitted in 6D using an invariant polynomial method[37,38]. The PES was expanded in the form,

$$V(y_1 \cdots y_6) = \sum_{n_1 \cdots n_6}^{N} c_{n_1 \cdots n_6} y_1^{n_1} y_6^{n_6} [y_2^{n_2} y_3^{n_3} y_4^{n_4} y_5^{n_5} + y_2^{n_5} y_3^{n_4} y_4^{n_3} y_5^{n_2}], \quad (3)$$

where $y_i = e^{-0.5 d_i}$ is a Morse-type variable. The internuclear distances d_i between two atoms are defined as $d_1 = d_{HH'}$, $d_2 = d_{OH'}$, $d_3 = d_{CH'}$, $d_4 = d_{CH}$, $d_5 = d_{OH}$ and $d_6 = d_{CO}$. The total power of the polynomial, $N = n_1 + n_2 + n_3 + n_4 + n_5 + n_6$, was restricted to a maximum of 6. Expansion coefficients $c_{n_1 \cdots n_6}$ were obtained using weighted least-squares fitting for potential energies up to 10,000 cm^{-1}. The RMS error in the fit of the PES is 14.22 cm^{-1}, which included 398,218 different geometries. This RMS error can be compared with that of 277 cm^{-1} for the 6D reactive surface of Zhang *et al.*[36] which, however, extended to more than 30,000 cm^{-1}. From the computed energy points, the global minimum of the total potential corresponds to the collinear arrangement H-H-C-O ($\theta_1 = 0, \theta_2 = 0, \phi = 0$) with a depth of -85.937 cm^{-1} at $R = 8.0$ a_0 with r_1 and r_2 at their, respectively, equilibrium positions. This compares with the global minimum of the interaction potential obtained by Jankowski *et al.*[35] from their fitted V12 PES averaged over r_1 and r_2: $R = 7.911$ a_0 and -93.651 cm^{-1}. Note that this comparison is only suggestive, as the global minimum in the total and interaction potentials coincide only when bond lengths (r_1 and r_2) are fixed at their equilibrium values as illustrated in Fig. 1 and that is not the case for V12.

Scattering theory and computational details. The quantum scattering theory for a collision of an S-state atom with a rigid-rotor was developed[2,57–59], based on the close-coupling (CC) formulation of Arthurs and Dalgarno[1]. Details about its extension to diatom–diatom collisions with full-vibrational motion can be found in refs 12,13. In this approach, the interaction potential $V(R, r_1, r_2, \theta_1, \theta_2, \phi)$ is expanded as,

$$V(R, r_1, r_2, \theta_1, \theta_2, \phi) = \sum_{\lambda_1 \lambda_2 \lambda_{12}} A_{\lambda_1, \lambda_2, \lambda_{12}}(r_1, r_2, R) Y_{\lambda_1, \lambda_2, \lambda_{12}}(\hat{r}_1, \hat{r}_2, \hat{R}), \quad (4)$$

with the bi-spherical harmonic function expressed as,

$$Y_{\lambda_1, \lambda_2, \lambda_{12}}(\hat{r}_1, \hat{r}_2, \hat{R}) = \sum_{m_{\lambda_1} m_{\lambda_2} m_{\lambda_{12}}} \langle \lambda_1 m_{\lambda_1} \lambda_2 m_{\lambda_2} \mid \lambda_{12} m_{\lambda_{12}} \rangle \times Y_{\lambda_1 m_{\lambda_1}}(\hat{r}_1) Y_{\lambda_2 m_{\lambda_2}}(\hat{r}_2) Y^*_{\lambda_{12} m_{\lambda_{12}}}(\hat{R}), \quad (5)$$

where $0 \leq \lambda_1 \leq 10$, $0 \leq \lambda_2 \leq 6$ was used in the scattering calculations. Owing to the symmetry of H_2, only even values of λ_2 contribute.

For convenience, the combined molecular state (CMS) notation is applied to describe a combination of rovibrational states for the two diatoms. A CMS represents a unique quantum state of the diatom–diatom system before or after a collision. The CMS will be denoted as ($v_1 j_1 v_2 j_2$). v and j are the vibrational and rotational quantum numbers.

The rovibrational state-to-state cross-section as a function of collision energy E is given by,

$$\sigma_{v_1 j_1 v_2 j_2, v_1' j_1' v_2' j_2'}(E) = \frac{\pi}{(2j_1 + 1)(2j_2 + 1) k^2} \times \sum_{j_{12} j_{12}' l l' J \varepsilon_l} (2J + 1) \mid \delta_{v_1 j_1 v_2 j_2 l, v_1' j_1' v_2' j_2' l'} - S^{J \varepsilon_l}_{v_1 j_1 v_2 j_2 l, v_1' j_1' v_2' j_2' l'}(E) \mid^2, \quad (6)$$

where ($v_1 j_1 v_2 j_2$) and ($v_1' j_1' v_2' j_2'$) are, respectively, the initial and final CMSs of CO–H_2, the wave vector $k^2 = 2\mu E/\hbar^2$ and S is the scattering matrix. l is the orbital angular momentum and J the total collision system angular momentum, where $\mathbf{J} = \mathbf{l} + \mathbf{j}_{12}$ and $\mathbf{j}_{12} = \mathbf{j}_1 + \mathbf{j}_2$.

Thorough convergence testing was performed in the scattering calculations by varying all relevant parameters. The CC equations were propagated for each value of R from 4 to 18.0 a_0 using the log-derivative matrix propagation method of Johnson[60] and Manolopoulos[61], which was found to converge for a radial step-size of $\Delta R = 0.05$ a_0. The convergence tests of the $v_1 = 1 \rightarrow 0$ vibrational quenching cross-section of CO with respect to the number of $v_1 = 1$ rotational channels found that at least 13–15 channels have to be included in the $v_1 = 1$ basis set, especially for low-energy scattering. On the basis of convergence tests with respect to the adopted maximum R for the long-range part of the PES, we found that the cross-sections are converged down to the lowest collision energy of 0.1 cm^{-1}. This value also guarantees that the rate coefficients are converged for temperatures >1 K. The number of discrete variable representation points N_{r1} and N_{r2}; the number of points in θ_1 and θ_2 for Gauss-Legendre quadrature, $N_{\theta 1}$ and $N_{\theta 2}$; and the number of points in ϕ for Gauss-Hermite quadrature, N_ϕ, which were applied to project out the potential expansion coefficients, were all tested for convergence with the final adopted values given in Supplementary Table 2. The basis sets and the maximum number of coupled channels are also presented in Supplementary Table 2.

The resulting integral cross-sections were thermally averaged over a Maxwellian kinetic energy distribution to yield state-to-state rate coefficients as function of temperature T,

$$k_{v_1 j_1 v_2 j_2, v_1' j_1' v_2' j_2'}(T) = \left(\frac{8}{\pi m \beta}\right)^{1/2} \beta^2 \int_0^\infty E \sigma_{v_1 j_1 v_2 j_2, v_1' j_1' v_2' j_2'}(E) \exp(-\beta E) dE, \quad (7)$$

where m is the reduced mass of the CO–H_2 complex, $\beta = (k_B T)^{-1}$ and k_B is Boltzmann's constant.

References

1. Arthurs, A. M. & Dalgarno, A. The theory of scattering by a rigid rotor. *Proc. R. Soc.* **A 256,** 540–551 (1960).

2. Takayanagi, K. The production of rotational and vibrational transitions in encounters between molecules. *Adv. Atom. Mol. Phys.* **1,** 149–194 (1965).
3. Dubernet, M.-L. *et al.* BASECOL2012: A collisional database repository and web service within the Virtual Atomic and Molecular Data Centre (VAMDC). *Astron. Astrophys.* **553,** A50 (2013).
4. Roueff, E. & Lique, F. Molecular excitation in the interstellar medium: recent advances in collisional, radiative, and chemical processes. *Chem. Rev.* **113,** 8906–8938 (2013).
5. Althorpe, S. C. & Clary, D. C. Quantum scattering calculations on chemical reactions. *Annu. Rev. Phys. Chem.* **54,** 493–529 (2003).
6. Bhattacharya, S., Panda, A. N. & Meyer, H.-D. Multiconfiguration time-dependent Hartree approach to study the OH + H_2 reaction. *J. Chem. Phys.* **132,** 214304 (2010).
7. Bhattacharya, S., Kirwai, A., Panda, A. N. & Meyer, H.-D. Full dimensional quantum scattering study of the CN + H_2 reaction. *J. Chem. Sci.* **124,** 65–73 (2012).
8. Pogrebnya, S. K. & Clary, D. C. A full-dimensional quantum dynamical study of vibrational relaxation in H_2 + H_2. *Chem. Phys. Lett.* **363,** 523–528 (2002).
9. Panda, A. N., Otto, F., Gatti, F. & Meyer, H.-D. Rovibrational energy transfer in ortho-H_2 + para-H_2 collisions. *J. Chem. Phys.* **127,** 114310 (2007).
10. Lin, S. Y. & Guo, H. Full-dimensional quantum wave packet study of collision-induced vibrational relaxation between para-H_2. *Chem. Phys.* **289,** 191–199 (2003).
11. Quéméner, G., Balakrishnan, N. & Krems, R. V. Vibrational energy transfer in ultracold molecule-molecule collisions. *Phys. Rev. A* **77,** 030704(R) (2008).
12. Quéméner, G. & Balakrishnan, N. Quantum calculations of H_2-H_2 collisions: from ultracold to thermal energies. *J. Chem. Phys.* **130,** 114303 (2009).
13. dos Santos, S. F. *et al.* Quantum dynamics of rovibrational transitions in H_2-H_2 collisions: Internal energy and rotational angular momentum conservation effects. *J. Chem. Phys.* **134,** 214303 (2011).
14. Wilson, R. W., Jefferts, K. B. & Penzias, A. A. Carbon monoxide in Orion nebula. *Astrophys. J.* **161,** L43–L44 (1970).
15. Narayanan, D. *et al.* The nature of CO emission from $z\sim$ 6 quasars. *Astrophys. J. Suppl. Ser.* **174,** 13–30 (2008).
16. Lupu, R. E., Feldman, P. D., Weaver, H. A. & Tozzi, G.-P. The fourth positive system of carbon monoxide in the Hubble Space Telescope spectra of comets. *Astrophys. J.* **670,** 1473–1484 (2007).
17. Swain, M. R. *et al.* Molecular signatures in the near-infrared dayside spectrum of HD 189733b. *Astrophys. J. Lett.* **690,** L114–L117 (2009).
18. González-Alfonso, E. *et al.* CO and H_2O vibrational emission toward Orion Peak 1 and Peak 2. *Astron. Astrophys.* **386,** 1074–1102 (2002).
19. Brown, J. M. *et al.* VLT-CRIRES survey of rovibrational CO emission from protoplanetary disks. *Astrophys. J.* **770,** 94 (2013).
20. Brittain, S. D., Najita, J. R. & Carr, J. S. Tracing the inner edge of the disk around HD 100546 with rovibrational CO emission lines. *Astrophys. J.* **702,** 85–99 (2009).
21. Bertelsen, R. P. H. *et al.* CO ro-vibrational lines in HD 100546: A search for disc asymmetries and the role of fluorescence. *Astron. Astrophys.* **561,** A102 (2014).
22. Patel, N. A. *et al.* Detection of vibrationally excited CO in IRC + 10216. *Astrophys. J.* **691,** L55–L58 (2009).
23. Thi, W. F. *et al.* Radiation thermo-chemical models of protoplanetary discs IV. Modelling CO ro-vibrational emission from Herbig Ae discs. *Astron. Astrophys.* **551,** A49 (2013).
24. Krems, R. V. *TwoBC - quantum scattering program* (University of British Columbia, 2006).
25. Bačić, Z., Schinke, R. & Diercksen, G. H. F. Vibrational relaxation of CO (n = 1) in collisions with H_2. I. Potential energy surface and test of dynamical approximations. *J. Chem. Phys.* **82,** 236–244 (1985).
26. Bačić, Z., Schinke, R. & Diercksen, G. H. F. Vibrational relaxation of CO (n = 1) in collisions with H_2. II. Influence of H_2 rotation. *J. Chem. Phys.* **82,** 245–253 (1985).
27. Reid, J. P., Simpson, C. J. S. M. & Quiney, H. M. The vibrational deactivation of CO(v = 1) by inelastic collisions with H_2 and D_2. *J. Chem. Phys.* **106,** 4931–4944 (1997).
28. Flower, D. R. Rate coefficients for the rovibrational excitation of CO by H_2 and He. *Mon. Not. R. Astron. Soc.* **425,** 1350–1356 (2012).
29. Andrews, A. J. & Simpson, C. J. S. M. Vibrational relaxation of CO by H_2 down to 73 K using a chemical CO laser. *Chem. Phys. Lett.* **36,** 271–274 (1975).
30. Andrews, A. J. & Simpson, C. J. S. M. Vibrational deactivation of CO by n-H_2, by p-H_2 and by HD measured down to 77 K using laser fluorescence. *Chem. Phys. Lett.* **41,** 565–569 (1976).
31. Wilson, G. J., Turnidge, M. L., Solodukhin, A. S. & Simpson, C. J. S. M. The measurement of rate constants for the vibrational deactivation of $^{12}C^{16}O$ by H_2, D_2 and ^4He in the gas phase down to 35 K. *Chem. Phys. Lett.* **207,** 521–525 (1993).
32. Schinke, R., Meyer, H., Buck, U. & Diercksen, G. H. F. A new rigid-rotor H_2-CO potential-energy surface from accurate ab initio calculations and rotationally inelastic-scattering data. *J. Chem. Phys.* **80,** 5518–5530 (1984).
33. Jankowski, P. & Szalewicz, K. Ab initio potential energy surface and infrared spectra of H_2-CO and D_2-CO van der Waals complexes. *J. Chem. Phys.* **108,** 3554–3565 (1998).
34. Jankowski, P. & Szalewicz, K. A new ab initio interaction energy surface and high-resolution spectra of the H_2-CO van der Waals complex. *J. Chem. Phys.* **123,** 104301 (2005).
35. Jankowski, P. *et al.* A comprehensive experimental and theoretical study of H_2-CO spectra. *J. Chem. Phys.* **138,** 084307 (2013).
36. Zhang, X., Zou, S., Harding, L. B. & Bowman, J. M. A global ab initio potential energy surface for formaldehyde. *J. Phys. Chem. A* **108,** 8980–8986 (2004).
37. Braams, B. J. & Bowman, J. M. Permutationally invariant potential energy surfaces in high dimensionality. *Int. Rev. Phys. Chem.* **28,** 577–606 (2009).
38. Bowman, J. M., Czakó, G. & Fu, B. N. High-dimensional ab initio potential energy surfaces for reaction dynamics calculations. *Phys. Chem. Chem. Phys.* **13,** 8094–8111 (2011).
39. Hutson, J. M. & Green, S. MOLSCAT computer code, Version 14 http://www.giss.nasa.gov/tools/molscat/ (1994).
40. Antonova, S., Tsakotellis, A. P., Lin, A. & McBane, G. C. State-to-state rotational excitation of CO by H_2 near 1000 cm^{-1} collision energy. *J. Chem. Phys.* **112,** 554–559 (2000).
41. Chefdeville, S. *et al.* Appearance of low energy resonances in CO-para-H_2 inelastic collisions. *Phys. Rev. Lett.* **109,** 023201 (2012).
42. Hooker, W. J. & Millikan, R. C. Shocktube study of vibrational relaxation in carbon monoxide for the fundamental and first overtone. *J. Chem. Phys.* **38,** 214–220 (1963).
43. Millikan, R. C. & Osburg, L. A. Vibrational relaxation of carbon monoxide by ortho- and para-hydrogen. *J. Chem. Phys.* **41,** 2196–2197 (1964).
44. Kobayashi, R., Amos, R. D., Reid, J. P., Quiney, H. M. & Simpson, C. J. S. M. Coupled cluster ab initio potential energy surfaces for CO…He and CO…H_2. *Mol. Phys.* **98,** 1995–2005 (2000).
45. Chandler, D. W. Cold and ultracold molecules: Spotlight on orbiting resonances. *J. Chem. Phys.* **132,** 110901 (2010).
46. Casavecchia, P. & Alexander, M. H. Uncloaking the quantum nature of inelastic molecular collisions. *Science* **341,** 1076–1077 (2013).
47. Henning, T. & Semenov, D. Chemistry in protoplanetary disks. *Chem. Rev.* **113,** 9016–9042 (2013).
48. Adler, T. B., Knizia, G. & Werner, H.-J. A simple and efficient CCSD(T)-F12 approximation. *J. Chem. Phys.* **127,** 221106 (2007).
49. Werner, H.-J., Adler, T. B. & Manby, F. R. General orbital invariant MP2-F12 theory. *J. Chem. Phys.* **126,** 164102 (2007).
50. Werner, H.-J. *et al.* MOLPRO, version 20101. A package of ab initio programs http://www.molpro.net.
51. Hill, J. G., Mazumder, S. & Peterson, K. A. Correlation consistent basis sets for molecular core-valence effects with explicitly correlated wave functions: The atoms B-Ne and Al-Ar. *J. Chem. Phys.* **132,** 054108 (2010).
52. Hättig, C. Optimization of auxiliary basis sets for RI-MP2 and RI-CC2 calculations: Core-valence and quintuple-zeta basis sets for H to Ar and QZVPP basis sets for Li to Kr. *Phys. Chem. Chem. Phys.* **7,** 59–66 (2005).
53. Weigend, F. A fully direct RI-HF algorithm: Implementation, optimised auxiliary basis sets, demonstration of accuracy and efficiency. *Phys. Chem. Chem. Phys.* **4,** 4285–4291 (2002).
54. Tew, D. P. & Klopper, W. A comparison of linear and nonlinear correlation factors for basis set limit Moller-Plesset second order binding energies and structures of He_2, Be_2, and Ne_2. *J. Chem. Phys.* **125,** 094302 (2006).
55. Feller, D., Peterson, K. A. & Hill, J. G. Calibration study of the CCSD(T)-F12a/b methods for C_2 and small hydrocarbons. *J. Chem. Phys.* **133,** 184102 (2010).
56. Bernardi, F. & Boys, S. F. Calculation of small molecular interactions by differences of separate total energies - some procedures with reduced errors. *Mol. Phys.* **19,** 553 (1970).
57. Green, S. Rotational excitation in H_2-H_2 collisions - close-coupling calculations. *J. Chem. Phys.* **62,** 2271–2277 (1975).
58. Alexander, M. H. & DePristo, A. E. Symmetry considerations in quantum treatment of collisions between two diatomic-molecules. *J. Chem. Phys.* **66,** 2166–2172 (1977).
59. Zarur, G. & Rabitz, H. Effective potential formulation of molecule-molecule collisions with application to H_2-H_2. *J. Chem. Phys.* **60,** 2057–2078 (1974).
60. Johnson, B. R. Multichannel log-derivative method for scattering calculations. *J. Comp. Phys.* **13,** 445–449 (1973).
61. Manolopoulos, D. E. An improved log derivative method for inelastic-scattering. *J. Chem. Phys.* **85,** 6425–6429 (1986).

Acknowledgements

Work at UGA and Emory was supported by NASA grant NNX12AF42G from the Astronomy and Physics Research and Analysis Program, at UNLV by NSF Grant No. PHY-1205838, and at Penn State by NSF Grant No. PHY-1203228. This study was supported in part by resources and technical expertise from the UGA Georgia Advanced Computing Resource Center (GACRC), a partnership between the UGA Office of the Vice President for Research and Office of the Vice President for Information Technology.

We thank Shan-Ho Tsai (GACRC), Jeff Deroshia (UGA Department of Physics and Astronomy) and Gregg Derda (GACRC) for computational assistance.

Author contributions

B.H.Y. performed the potential energy surface (PES) fitting and scattering calculations. P.Z. calculated the PES. X.W. and J.M.B. developed the PES fitting code. N.B., R.C.F., and P.C.S. extended and modified the TwoBC code for CO–H_2 rovibrational scattering calculations, while N.B. assisted with the scattering calculations. B.H.Y., P.C.S. and P.Z. wrote the article with contributions from all other authors.

Additional information

Supplementary Information accompanies this paper at http://www.nature.com/naturecommunications

Competing financial interests: The authors declare no competing financial interests.

Reprints and permission information is available online at http://npg.nature.com/reprintsandpermissions/

How to cite this article: Yang, B.H. *et al.* Quantum dynamics of CO-H_2 in full dimensionality. *Nat. Commun.* 6:6629 doi: 10.1038/ncomms7629 (2015).